# Hyperbolic Positioning and Tracking of Moving UHF-RFID Tags by Exploiting Neural Networks

Spyros Megalou*, Aristidis Raptopoulos Chatzistefanou*, Anastasios Tzitzis*, Andreana Malama*, Traianos Yioultsis*, Antonis G. Dimitriou*
*School of ECE, Aristotle University of Thessaloniki, Thessaloniki, Greece, e-mail: antodimi@auth.gr

***Abstract*—In this paper we propose a novel real-time tracking method of a moving UHF-RFID tag. Two antenna pairs fixed at predefined positions monitor the moving tag collecting phase measurements. Phase differences are calculated for each pair and then mapped to distance-differences of the two antennas from the target tag. The latter corresponds to a hyperbola for each pair of antenna. The intersection of the two hyperbolas denotes the position of the tag. Since solving the system of hyperbolas to find the intersection point is not feasible with standard practices, a neural network is exploited to approximate the solution. Compared to prior art, the proposed method does not require knowledge of the tag's initial position or the trace followed (e.g. conveyor belt). Experiments were conducted by placing a tag on a moving robot capable of performing SLAM (Simultaneous Localization and Mapping) to know the ground truth. The results showed a mean error under 0.5m throughout the experimental campaign.**

***Index Terms*—RFID, tracking, hyperbolic positioning, phase, neural network**

## I. Introduction

The Fourth Industrial Revolution is starting to change our everyday life in a lot of its aspects. On this ongoing automation of traditional manufacturing, processing of goods, and industrial practices, Radio Frequency Identification(RFID) technology plays a significant role. An important part of RFID in this revolution is the localization and tracking of objects or humans. From tagging goods to empower logistics operations, to tagging humans to enhance security or provide statistics of visiting patterns, finding ways to track a moving RFID tag is of great importance.

In this paper the target is to track a visitor in the Archaeological Museum of Thessaloniki. Upon entrance, the visitors are given a ticket with an attached RFID tag. Antennas and readers are set at known locations in the museum collecting phase and RSSI measurements associated with each RFID tag. The phase data are exploited to track the moving tag thus quantify the behaviour of visitors and provide the staff of the museum with traffic statistics helping them to improve the experience of visitors.

A majority of approaches exist regarding RFID tag tracking in prior art. In [1], [2] and [3] RSSI data are exploited to track the tag. Received signal strength though is not a reliable indicator due to the fact that it is distorted from environmental factors such as multipath and shadowing, thus reducing the accuracy of the positioning. Other methods such as [4] and [5] take advantage of angle of arrival (AOA) data calculated from measurements collected from multiple antennas. In [4] the trace of the tag is known a priori, as the authors want to track the tag on a conveyor belt while in [5] the authors surround the target tags with three self-designed element antenna arrays to localize the tag. Authors in [6], [7] and [8] exploit phase measurements to track a moving tag. However the initial position of the tag must be known beforehand. Tagoram [9] is also a method that utilizes the phase of arrival (POA) of the signal to localize a moving tag and it does not depend on the initial position of the tag. However, Tagoram's complexity demands calculations that cannot be applied in real time.

In this work we develop a tracking technique that can track a moving tag in real time. The goal is to track visitors inside a museum and quantify their behaviour (i.e. duration of visit per exhibit etc.). Taking into consideration the layout of the museum and the arrangement of the exhibits the accuracy should be better than 1m. The initial position of the visitor is not known. The equipment used includes commercial of the shelf readers, antennas and tags.

## II. Proposed tracking method

The proposed method is able to track a moving or a stationary RFID tag. POA measurements are collected from 4 antennas (2 antenna pairs) which are located at predefined fixed positions. The phase data are collected from a single reader and the phase differences from the two antenna pairs are mapped to distance-differences to locate the moving tag. The proposed tracking technique can be analysed to the following 3 basic principles:

1) The RFID reader reports phase measurements from each antenna. Since the measurements are not collected at the same time, "common" time phase measurements are created via interpolation. Then phase differences for both antenna pairs are calculated and unwrapped.
2) The two phase-differences of the antenna pairs are translated to distance-difference curves. These curves are in fact two hyperbolas' branches which cross at the position of the tag. The foci of the hyperbolas are the positions of the two antennas of each pair.
3) Solving the system of hyperbolas' equations is not feasible with standard practices. To surpass this problem a deep neural network is trained with theoretical data creating a function which fits the solution of the system of hyperbolas for each point at the area of interest. The measurements collected by the reader pass through

the trained neural model and the position of the tag is estimated rapidly.

Let $\phi_i$ be the phase measured from antenna i denoted as:

$$\phi_i = (\phi^i_{prop} + \phi^i_o + \phi^i_{noise}) mod(2\pi), \quad (1)$$

$$\phi_{noise} \sim \mathcal{N}(0,\, \sigma^2_{phase})\,. \quad (2)$$

where $i$ is an index for each antenna (i.e. 1, 2, 3 and 4), $\phi^i_o$ is the phase offset including phases of the cables and other hardware and $\phi^i_{noise}$ is the measurement's noise. Phase $\phi^i_{prop}$ corresponds to the phase accumulated due to the round trip of the electromagnetic wave and is given by[10]:

$$\phi^i_{prop} = \frac{4\pi}{\lambda} ||\mathbf{A}_{tag} - \mathbf{A}^i_{ant}||_2 = \frac{4\pi d_i}{\lambda}, \quad (3)$$

where $||\mathbf{A}_{tag} - \mathbf{A}^i_{ant}||_2$ denotes the euclidean distance between the tag and the reader's antenna:

$$||\mathbf{A}_{tag} - \mathbf{A}^i_{ant}||_2 = \sqrt{(x_{tag} - x_i)^2 + (y_{tag} - y_i)^2}, \quad (4)$$

Phase measurements reported by the reader are collected at different time instances for different antennas. To calculate the phase differences between the antennas a common time series is generated according to the time instances of the raw phase measurements. The common time instances are generated via linear interpolation at time slots where a high read rate per tag is observed. For all common time instances $t$, phase differences $\Delta\phi_{12,t}$ and $\Delta\phi_{34,t}$ are calculated as:

$$\Delta\phi_{12,t} = \phi_{1,t} - \phi_{2,t} \quad \text{and} \quad \Delta\phi_{34,t} = \phi_{3,t} - \phi_{4,t} \quad (5)$$

The two phase differences are then mapped to distance-differences. Without loss of generality let's assume a multipath and noise free environment and that the phase measurements are unwrapped. By substituting (1) and (3) to (5) the phase differences for antenna pairs $1-2$ and $3-4$ are given by:

$$\Delta\phi_{12} = \frac{4\pi}{\lambda}(d_1 - d_2) \quad \text{and} \quad \Delta\phi_{34} = \frac{4\pi}{\lambda}(d_3 - d_4) \quad (6)$$

$$\Rightarrow \quad \Delta d_{12} = \frac{\lambda}{4\pi}\Delta\phi_{12} \quad \text{and} \quad \Delta d_{34} = \frac{\lambda}{4\pi}\Delta\phi_{34} \quad (7)$$

Equations (6) and (7) show that the range of phase difference of an antenna-pair, depends on the distance between the two antennas. The maximum phase difference is observed when $d_1 - d_2$ is maximized. As shown in Fig. 1 this happens when the tag's position is on the line connecting the center of the two antennas(i.e. when $d_1 - d_2 = d_{12}$).

If $d_{12} = \lambda/2$ then the calculated phase difference ranges between $-2\pi$ to $2\pi$. In this work the distance between the antennas for each pair is considered less than $\lambda/2$.

By substituting (4) in (7) we get:

$$||\mathbf{A}_{tag} - \mathbf{A}^1_{ant}||_2 - ||\mathbf{A}_{tag} - \mathbf{A}^2_{ant}||_2 = \frac{\lambda}{4\pi}\Delta\phi_{12} \quad (8)$$

$$||\mathbf{A}_{tag} - \mathbf{A}^3_{ant}||_2 - ||\mathbf{A}_{tag} - \mathbf{A}^4_{ant}||_2 = \frac{\lambda}{4\pi}\Delta\phi_{34} \quad (9)$$

As shown in Fig. 2 the loci of (8) and (9) are two hyperbolas intersecting in the actual position of the tag, assuming noiseless line of sight measurements.

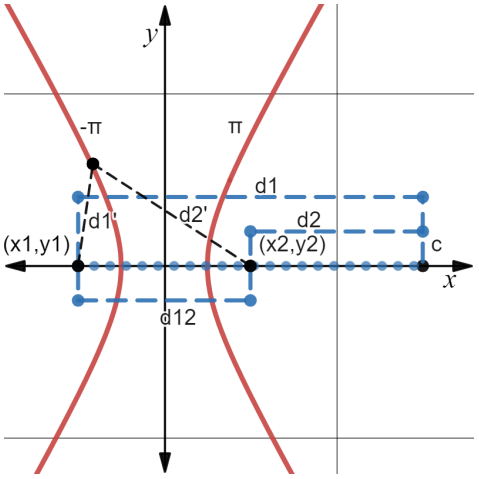


Fig. 1. Two antennas are located in $(x_1, y_1)$ and $(x_2, y_2)$ accordingly. Maximum phase difference is observed on the line connecting the two points where $d = d_1 - d_2 \Rightarrow d = d_{12}$.

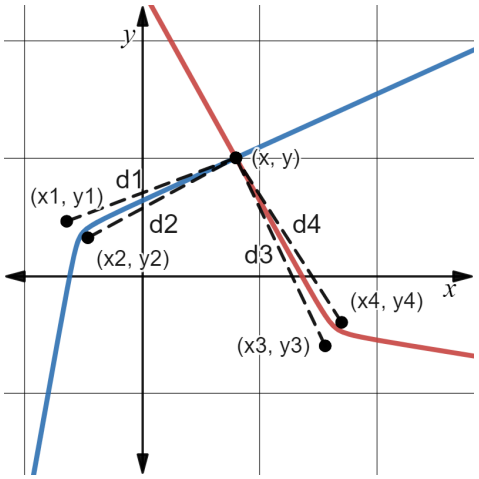


Fig. 2. Point of intersection of two hyperbolas in the general case.

To estimate the position of the tag $\mathbf{A}_{tag}$ need to be solved. Trying to solve the system of equations (8) and (9) to estimate the tag's position leads to sextic polynomials. This type of polynomials cannot be solved with standard practices in the general case. To overcome this problem a deep neural network has been trained to approximate the solution of this system. The phase differences of the two antenna pairs are the input of the neural model and the tag's position the output.

By training the model with the unwrapped phase differences of the actual geometry, we make sure that there exists a 1 - 1 mapping between a pair of signed phase differences and a unique location in the area of interest. If the distance between the antennas, in the actual setup, is such, that many hyperbolas should be considered among each antenna-pair, due to phase wrapping of the measurements, all we have to do is feed the trained neural network with all possible unwrapped phase differences and it will output all possible locations of the target in the area of interest.

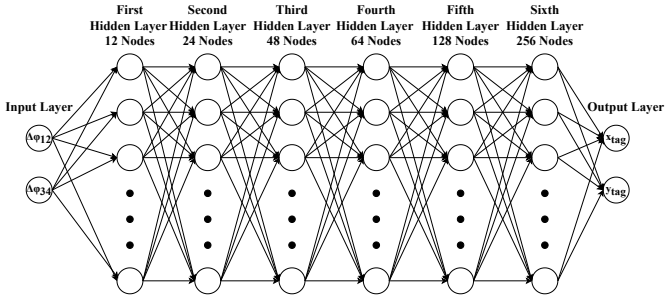


Fig. 3. The architecture of the Neural Network

The trained model is basically a function expressed as:

$$F_{NN}(\Delta\phi_{12}, \Delta\phi_{34}) = \mathbf{A}_{tag} \tag{10}$$

The neural network is designed as a multilayer perceptron (MLP) and its main goal is to approximate a function. A representation of the MLP designed, is shown in Fig. 3. The MLP consists of two input nodes ($\Delta\phi_{12}, \Delta\phi_{34}$), 5 hidden layers (12, 24, 48, 64, 128 and 256 nodes respectively) and two output nodes ($x_{tag}, y_{tag}$). A ReLu activation function was used for all layers and RMSProp for the optimizer. To enhance the training of the model a custom loss function was selected and is given by:

$$Loss = ||\mathbf{A}_{tag\_real} - \mathbf{A}_{tag\_est}|| \tag{11}$$

The neural network training process can be decomposed in the following steps:

1) The area of interest is mapped and a coordinate system is defined.
2) Arrangement of the antenna-pairs is decided, taking into consideration coverage and minimization of intersection points of the hyperbolas' branches.
3) For the given area, a dense grid of $1x1cm^2$ is assigned. The density of the grid varies with respect to the desired accuracy of the tracking method.
4) The theoretical values of the unwrapped phase differences for each antenna pair are calculated. These phase differences along with the corresponding grid points form the training data set.
5) The neural model is trained until a predefined threshold of mean error and standard deviation is passed (e.g. $\mu_{error} < 0.02m$ and $\sigma^2_{error} < 0.01m$).

## III. Performance of Tracking Algorithm in Experimental Setup

The experiments took place in a lab of the School of Electrical and Computer Engineering of Aristotle University of Thessaloniki. As shown in Fig. 4 the target-tag is attached on a robot capable of performing SLAM. This allows us to know the exact position of the tag in the search area. For phase data measurements an Impinj Speedway R420 reader was used and four Laird PER86506 antennas. To imitate a movement of a human the speed of the robot does not remain

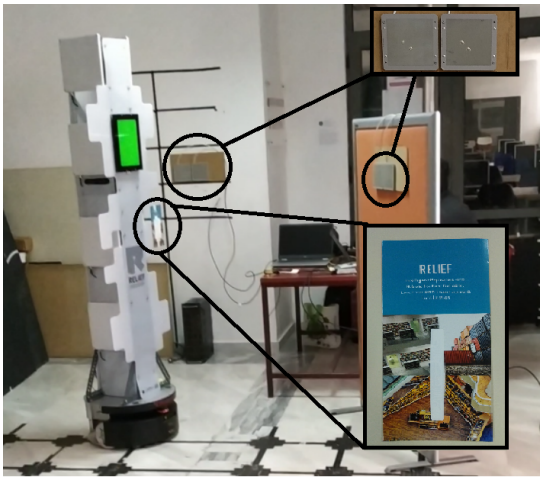


Fig. 4. The setup of the experiments. The tag is placed on a robot able to perform SLAM. The two antenna pairs are placed at known locations and the two antennas per pair are placed at a distance less than $\lambda/2$.

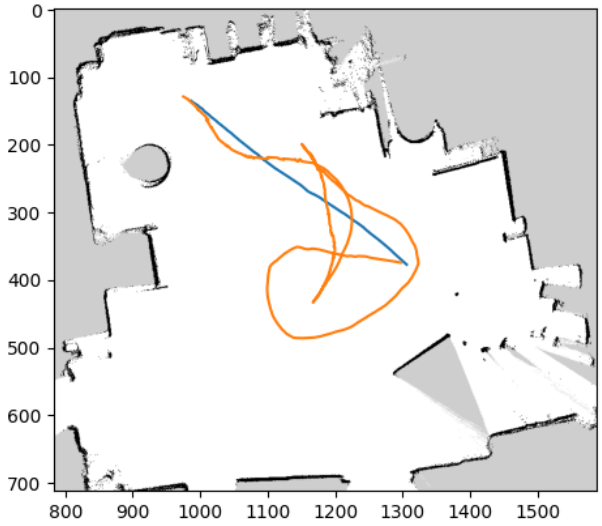


Fig. 5. The two paths followed by the tag on the robot during experiments. The blue path is a straight path without stops and changes on the speed of the robot while the orange path imitates a human movement as the robot decelerates turns arbitrarily and performs stops along the route followed.

constant through out the experiments. The robot accelerates, decelerates or even stops. The map of the experiments' setup and the tag's trajectories are shown in Fig. 5.

Fig. 6 shows the steps of the tracking algorithm for the random path, since it is more representative of a visitor's behaviour. Each subfigure represents a step of the algorithm. For the selected space and antenna locations a neural network is trained to calculate the position of a tag.

Phase data are collected from each antenna and common time measurements are created via linear interpolation (Fig. 6a). Then, the phase differences are calculated and the unwrapping process take place ( 6b). The phase data collected are wrapped. As result, the sign of the collected phase difference is ambiguous. Given that the distance between the antennas

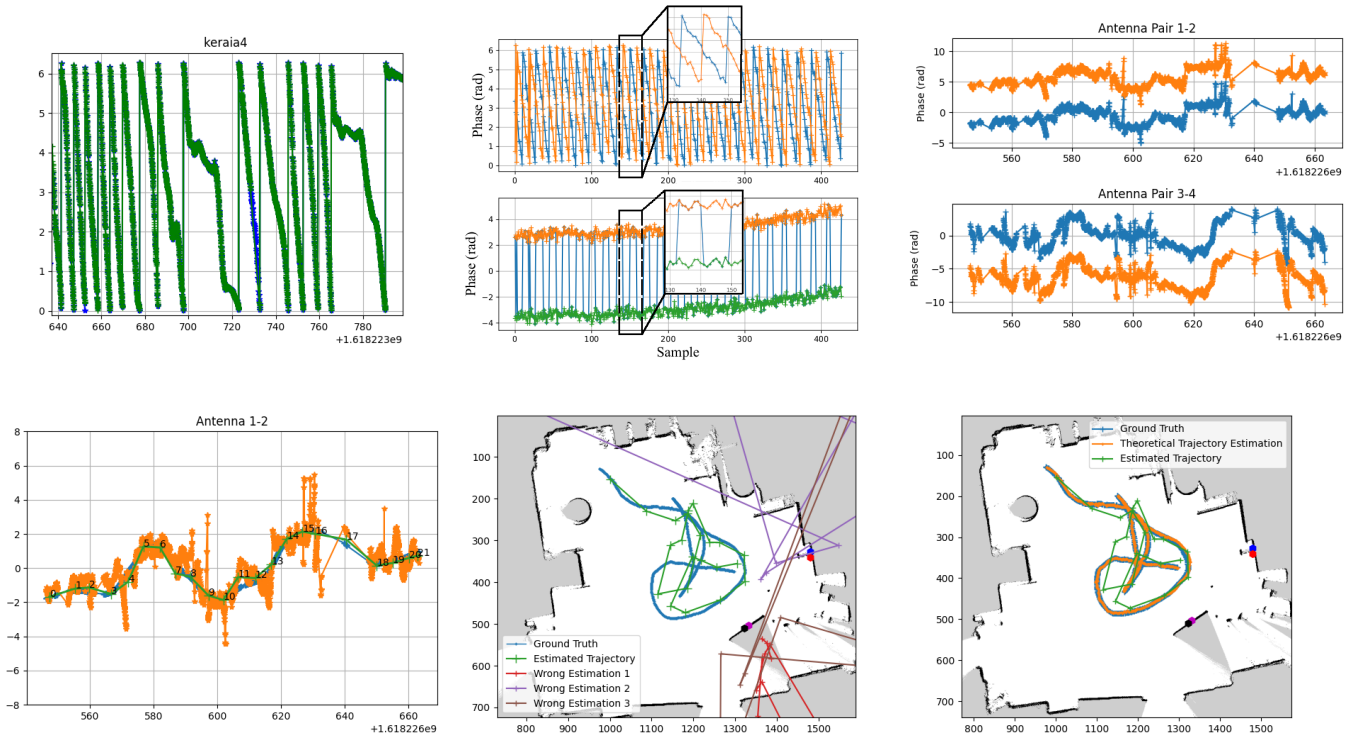


Fig. 6. Steps of the Tracking Algorithm.

on each pair is less than $\lambda/2$, two possible phase difference sequences are generated for each antenna pair.

This leads to two possible sequences of phase differences for both antenna pairs. The same ambiguity exists also on the other antenna pair, creating 4 possible combinations of sequences in total, hence 4 possible trajectories. In case of Fig. 6c the two possible sequences for antenna pair 1-2 and 3-4 can be seen with the orange and blue color in the two subplots respectively.

As shown in Fig. 6c the phase difference sequences are distorted by noise and multipath. To overcome this distortion an average of consecutive phase measurements in a time window of 5 seconds is calculated (Fig. 6d).

The four phase difference sequences generate four possible trajectories after passing through the trained model. The trajectories that either exceed the area's boundaries or present steps bigger than a human could possible perform during 5 seconds, are rejected(red, brown and purple paths in Fig. 6e). After the trajectory rejection process, the final estimated trajectory is presented in Fig. 6f.

To evaluate the performance of the tracking method the mean error is calculated which is given by:

$$Error = \frac{\sum_{n=1}^{N} ||\mathbf{A}^n_{tag\_est} - \mathbf{A}^n_{tag\_real}||_2}{N} \qquad (12)$$

The resultant error for the straight and the random paths of Fig. 5 were 0.24m and 0.47m respectively. Additional experiments were conducted, deploying the same setup, but forcing the robot to move along different trajectories. The mean error was kept below 0.5m in all cases.

## IV. Conclusion

Real-time tracking of moving targets is a key feature for Industry 4.0 applications. In this paper we present a novel method on tracking a UHF-RFID tagged target in real time. The method exploits neural networks to perform hyperbolic positioning of the tag in the search area given. The proposed neural model needs to be trained only once for each antenna-geometry installation. It is trained until reaching low values of mean error and std. A priori knowledge of initial position of the target is not needed. The tracking method will be used to track visitors inside a museum and quantify their behaviour. The authors believe that the proposed tracking method can be used for a majority of indoor or outdoor RFID tracking applications. The results of experiments show that the mean error remains under 0.5m even in arbitrary movements of the tag.

Future work includes more experiments in different environments and larger tag populations to test the robustness of the algorithm in different multipath scenarios. Also experiments where the tag is placed on a human will be held to investigate the effect of human body on the phase measurements and consequently to the accuracy of the method.

## Acknowledgment

This research has been co-financed by the European Union and Greek national funds through the Operational Program Competitiveness, Entrepreneurship and Innovation, under the call RESEARCH – CREATE – INNOVATE (project code: T2EDK-02000).

## REFERENCES


[1] T. Kanda, M. Shiomi, L. Perrin, T. Nomura, H. Ishiguro and N. Hagita, "Analysis of People Trajectories with Ubiquitous Sensors in a Science Museum," Proceedings 2007 IEEE International Conference on Robotics and Automation, 2007, pp. 4846-4853, doi: 10.1109/ROBOT.2007.364226.

[2] A. R. Jimenez Ruiz, F. Seco Granja, J. C. Prieto Honorato and J. I. Guevara Rosas, "Accurate Pedestrian Indoor Navigation by Tightly Coupling Foot-Mounted IMU and RFID Measurements," in IEEE Transactions on Instrumentation and Measurement, vol. 61, no. 1, pp. 178-189, Jan. 2012, doi: 10.1109/TIM.2011.2159317.

[3] M. Omer, G. Y. Tian, "Indoor distance estimation for passive UHF RFID tag based on RSSI and RCS," Measurement, Volume 127, pp. 425-430, 2018, doi:10.1016/j.measurement.2018.05.116.

[4] Y. Zhang, M. G. Amin, S. Kaushik, "Localization and Tracking of Passive RFID Tags Based on Direction Estimation," International Journal of Antennas and Propagation, vol. 2007, doi: 10.1155/2007/17426.

[5] S. Azzouzi, M. Cremer, U. Dettmar, R. Kronberger and T. Knie, "New measurement results for the localization of UHF RFID transponders using an Angle of Arrival (AoA) approach," 2011 IEEE International Conference on RFID, 2011, pp. 91-97, doi: 10.1109/RFID.2011.5764607.

[6] X. Lu, L. Wang, D. Zhao and C. Zhai, "Multi-tag RFID system enables localization and tracking," Journal of Physics: Conference Series, vol. 1168, 2019, doi:10.1088/1742-6596/1168/2/022103.

[7] S. Sarkka, V. V. Viikari, M. Huusko and K. Jaakkola, "Phase-Based UHF RFID Tracking With Nonlinear Kalman Filtering and Smoothing," in IEEE Sensors Journal, vol. 12, no. 5, pp. 904-910, May 2012, doi: 10.1109/JSEN.2011.2164062.

[8] C. Jiang, Y. He, X. Zheng and Y. Liu, "Orientation-Aware RFID Tracking with Centimeter-Level Accuracy," 2018 17th ACM/IEEE International Conference on Information Processing in Sensor Networks (IPSN), 2018, pp. 290-301, doi: 10.1109/IPSN.2018.00057.

[9] L. Yang, Y. Chen, X. Y. Li, Ch. Xiao, Mo Li and Y. Liu, "Tagoram: Real-time Tracking of Mobile RFID tags to High Precision Using COTS Devices," 2014, 20th Annual International Conference on Mobile Computing and Networking (MobiCom '14), 2014, pp 237–248, doi: 10.1145/2639108.2639111.

[10] P. V. Nikitin, R. Martinez, S. Ramamurthy, H. Leland, G. Spiess and K. V. S. Rao, "Phase based spatial identification of UHF RFID tags," 2010 IEEE International Conference on RFID (IEEE RFID 2010), 2010, pp. 102-109, doi: 10.1109/RFID.2010.5467253.